

9-15-2017

GUCY2C Signaling Opposes the Acute Radiation-Induced GI Syndrome.


Peng Li
University of Florida

Evan Wuthrick
Ohio State University Comprehensive Cancer Center

Jeff A. Rappaport
Thomas Jefferson University

Crystal Kraft
Thomas Jefferson University

Jieru E. Lin
Follow this and additional works at: <https://jdc.jefferson.edu/petfp>
Thomas Jefferson University

 Part of the [Medical Pharmacology Commons](#)

[Let us know how access to this document benefits you](#)

See next page for additional authors

Recommended Citation

Li, Peng; Wuthrick, Evan; Rappaport, Jeff A.; Kraft, Crystal; Lin, Jieru E.; Marszalowicz, Glen; Snook, Adam E.; Zhan, Tingting; Hyslop, Terry M.; and Waldman, Scott A., "GUCY2C Signaling Opposes the Acute Radiation-Induced GI Syndrome." (2017). *Department of Pharmacology and Experimental Therapeutics Faculty Papers*. Paper 87.
<https://jdc.jefferson.edu/petfp/87>

This Article is brought to you for free and open access by the Jefferson Digital Commons. The Jefferson Digital Commons is a service of Thomas Jefferson University's [Center for Teaching and Learning \(CTL\)](#). The Commons is a showcase for Jefferson books and journals, peer-reviewed scholarly publications, unique historical collections from the University archives, and teaching tools. The Jefferson Digital Commons allows researchers and interested readers anywhere in the world to learn about and keep up to date with Jefferson scholarship. This article has been accepted for inclusion in Department of Pharmacology and Experimental Therapeutics Faculty Papers by an authorized administrator of the Jefferson Digital Commons. For more information, please contact: JeffersonDigitalCommons@jefferson.edu.

Authors

Peng Li, Evan Wuthrick, Jeff A. Rappaport, Crystal Kraft, Jieru E. Lin, Glen Marszalowicz, Adam E. Snook, Tingting Zhan, Terry M. Hyslop, and Scott A. Waldman

<Research Article>

GUCY2C signaling opposes the acute radiation-induced GI syndrome

Peng Li¹, Evan Wuthrick², Jeff A. Rappaport³, Crystal Kraft³, Jieru E. Lin³, Glen Marszalowicz³, Adam E. Snook³, Tingting Zhan⁴, Terry M. Hyslop⁵, Scott A. Waldman³

¹Department of Pathology, Immunology and Laboratory Medicine, College of Medicine, The University of Florida, Gainesville, FL; ²Department of Radiation Oncology, The Ohio State University Comprehensive Cancer Center, Columbus, OH; ³Department of Pharmacology and Experimental Therapeutics, Divisions of Clinical Pharmacology and ⁴Biostatistics, Thomas Jefferson University, Philadelphia, PA; ⁵Department of Biostatistics and Bioinformatics, Duke University, Durham, NC.

RUNNING TITLE: GUCY2C opposes radiation-induced GI syndrome

Supported by grants to S.A. Waldman from NIH (R01 CA204881, R01 CA206026) and Targeted Diagnostic and Therapeutics Inc., and to the Kimmel Cancer Center of Thomas Jefferson University (P30 CA56036). P. Li and J.E. Lin were supported by NIH institutional award T32 GM08562 for Postdoctoral Training in Clinical Pharmacology. J.E. Lin is the recipient of the Young Investigator Award from the American Society for Clinical Pharmacology and Therapeutics (ASCPT). S.A. Waldman is the Samuel MV Hamilton Professor of Medicine at Thomas Jefferson University.

Correspondences: Scott A. Waldman, 1020 Locust Street, 368 JAH, Philadelphia, PA 19107; 215-955-5693; scott.waldman@jefferson.edu

Conflict of Interest: SAW is the Chair of the Data Safety Monitoring Board for the Chart-1 Trial™ sponsored by Cardio3 Biosciences, and the Chair (uncompensated) of the Scientific Advisory Board of Targeted Diagnostics & Therapeutics, Inc. which provided research funding that, in part, supported this work and has a license to commercialize inventions related to this work.

MANUSCRIPT METRICS

Title (with spaces):	64 characters
Running Title (with spaces):	44 characters
Abstract:	215 words
Text:	4,771 words
References:	55
Figures:	5
Tables:	0
Supplementary Materials:	Yes

Abstract

High doses of ionizing radiation induce acute damage to epithelial cells of the gastrointestinal (GI) tract, mediating toxicities restricting the therapeutic efficacy of radiation in cancer and morbidity and mortality in nuclear disasters. No approved prophylaxis or therapy exists for these toxicities, in part reflecting an incomplete understanding of mechanisms contributing to the acute radiation-induced GI syndrome (RIGS). Guanylate cyclase C (GUCY2C) and its hormones guanylin and uroguanylin have recently emerged as one paracrine axis defending intestinal mucosal integrity against mutational, chemical, and inflammatory injury. Here, we reveal a role for the GUCY2C paracrine axis in compensatory mechanisms opposing RIGS. Eliminating GUCY2C signaling exacerbated RIGS, amplifying radiation-induced mortality, weight loss, mucosal bleeding, debilitation and intestinal dysfunction. Durable expression of GUCY2C, guanylin and uroguanylin mRNA and protein by intestinal epithelial cells was preserved following lethal irradiation inducing RIGS. Oral delivery of the heat-stable enterotoxin (ST), an exogenous GUCY2C ligand, opposed RIGS, a process requiring p53 activation mediated by dissociation from MDM2. In turn, p53 activation prevented cell death by selectively limiting mitotic catastrophe, but not apoptosis. These studies reveal a role for the GUCY2C paracrine hormone axis as a novel compensatory mechanism opposing RIGS, and they highlight the potential of oral GUCY2C agonists (*LinzessTM*; *TrulanceTM*) to prevent and treat RIGS in cancer therapy and nuclear disasters.

Introduction

Exposure to radiation in the context of terrorist attacks or natural disasters produces death within about 10 days reflecting toxicity to the gastrointestinal (GI) tract, constituting the acute radiation-induced GI syndrome (RIGS) (1-3). In contrast to radiation-induced bone marrow toxicity, in which death can be prevented by bone marrow transplantation, there are no approved management paradigms to prevent or treat RIGS (4). Importantly, radiation therapy remains a mainstay in the management of cancer, a leading cause of death worldwide. Radiation therapy destroys rapidly proliferating cancer cells and, inevitably, normal tissues characterized by continuous regeneration programs, including hair follicles, bone marrow, the GI tract as well as other glandular epithelia (5). In that context, dose-limiting toxicities of radiation discourage patients from completing therapy; restrict maximum doses of radiation which limits the efficacy of treatment; and can lead to chronic morbidity and mortality (5).

Inadequate management in part reflects an incomplete understanding of mechanisms underlying RIGS. Indeed, critical molecular mechanisms and cellular targets mediating epithelial toxicity underlying RIGS remain controversial (6-14). Recent studies suggest that p53 in intestinal epithelial cells principally controls radiation-induced GI toxicity in mice, independently of apoptosis (7). In that context, deletion of the intrinsic apoptotic pathway from intestinal endothelial or epithelial cells failed to protect mice from GI toxicity-related death (7). In contrast, tissue-specific targeted deletion of intestinal epithelial cell p53 exacerbates, while its over-expression rescues, RIGS in mice (7,14). However, mechanisms underlying radiation-induced intestinal epithelial cell death and intestinal mucosa damage remain undefined (7).

GUCY2C is the intestinal receptor for the endogenous paracrine hormones guanylin (GUCA2A)

and uroguanylin (GUCA2B) and the heat-stable enterotoxins (STs) produced by diarrheagenic bacteria (15-17). This signaling axis plays a central role in mucosal physiology, regulating fluid and electrolyte secretion (15,16), and in coordinating crypt-surface homeostasis, regulating enterocyte proliferation, differentiation, metabolism, apoptosis, DNA repair, and epithelial-mesenchymal cross-talk (18-20). Further, this axis maintains the intestinal barrier, opposing epithelial injury induced by carcinogens, inflammation, and radiation, and its dysfunction contributes to the pathophysiology of inflammatory bowel disease and tumorigenesis (19-30). While the GUCY2C signaling axis has emerged as one guardian of intestinal epithelial integrity, the role of this axis in responses to lethal radiation, and its utility as a therapeutic target to prevent and treat RIGS remains undefined (22).

Here, we define a novel role for the GUCY2C paracrine hormone axis in compensatory responses opposing RIGS. Indeed, eliminating GUCY2C signaling amplifies radiation-induced GI toxicity. In that context, durable expression of GUCY2C, GUCA2A, and GUCA2B mRNA and protein is preserved following high doses of radiation that induce RIGS. Moreover, oral administration of the GUYC2C ligand ST opposed RIGS through a p53-dependent mechanism associated with the rescue of intestinal epithelial cells selectively from mitotic catastrophe, but not from apoptosis. These observations reveal a previously unrecognized compensatory mechanism to epithelial injury induced by high-dose radiation, involving signaling by the GUCY2C paracrine axis that opposes RIGS. They highlight the potential for oral GUCY2C-targeted agents to prevent or treat RIGS in the setting of cancer radiotherapy or environmental exposure through nuclear accident or terrorism. The opportunity to immediately translate these approaches is underscored by the recent regulatory approval of linaclotide (*Linzess™*) and plecanatide (*Trulance™*), oral GUCY2C

ligands that treat chronic constipation (31).

Materials and Methods

Animal models

Mice with a targeted germline deletion of GUCY2C (*Gucy2c*^{-/-}) are well-characterized, and were used after ≥ 14 generations of backcrossing onto the C57BL/6 background (15,16,18-20,26,32). *p53*^{FL}-*vil*-*Cre-ER*^{T2} mice were generated by crossbreeding *vil*-*Cre-ER*^{T2} (provided by S. Robine, Institut Curie-CNRS, France) with *p53*^{FL} transgenic mice (mixed FVB.129 and C57BL/6 backgrounds, kindly provided by Dr. Karen Knudsen, Thomas Jefferson University, Philadelphia, PA). Biallelic loss of p53 in intestinal epithelial cells (*p53*^{int}^{-/-}) was induced by IP administration of tamoxifen (75 mg tamoxifen/kg/d x 5 d) to F2 *p53*^{FL}-*vil*-*Cre-ER*^{T2} and control littermate *p53*⁺-*vil*-*Cre-ER*^{T2}, and deletion confirmed structurally by immunoblot analysis of phosphorylated p53 (pp53; Supplementary Fig. 1) and functionally by radiation-induced mortality (Supplementary Fig. 2). All experiments were carried out with mice that were between 2 to 3.5 months old (mixed males and females) and all mice were on mixed genetic backgrounds as described above and in Supplementary Figure 3. Where appropriate, age-matched and littermate controls were utilized to minimize the effect of genetic backgrounds. C57BL/6 mice used in oral ST or control peptide supplementation studies were obtained from NIH (NCI-Frederick) while those used for GUCY2C and ligand expression analysis were obtained from the Jackson Laboratory (Bar Harbor, ME). This study was approved by the Institutional Animal Care and Use Committee of Thomas Jefferson University (protocol 01518).

Gamma irradiation-induced GI toxicity

Anesthetized mice were irradiated with total-body gamma irradiation (TBI) or with back limbs to

tail and front limbs to head shielded with lead covers for subtotal-body irradiation (STBI) with exposure of abdominal area (approximately 1 inch² from xiphoid to pubic symphysis). Mice were irradiated with a ¹³⁷Cs irradiator (Gammacell 40) at a dose rate of approximately 70 cGy/min for different doses from 8 to 25 Gy/mice. Mice had free access to regular food and water before and after irradiation. The severity of GI toxicity was evaluated by mortality, debilitation (untidy fur coats), body weight, visible diarrhea, fecal occult blood, stool formation, stool water accumulation, and histopathology.

ST and control peptides

ST1-18 and control peptide (CP; inactive ST analog contains the same primary amino acid sequence, but with cysteines at positions 5, 6, 9, 10, 14, 17 replaced by alanine) were purchased from Bachem Co. (customer order; purity > 99.0%). ST and control peptides were resuspended in 1 X phosphate-buffered saline (PBS) at a concentration of 50 ng/μL. Mice were orally gavaged with 10 μg of CP or ST (in 200 μL solution) using a feeding needle (cat. # 01-208-88, Fisher Scientific) (26) daily for 14 d before and 14 d after irradiation. ST and CP were prepared by solid phase synthesis and purified by reverse phase HPLC, their structure confirmed by mass spectrometry by Bachem Co. (customer order; purity > 99.0%), and their activities confirmed by quantifying competitive ligand binding, guanylate cyclase activation and secretion in the suckling mouse assay (16,33).

Reagents

McCoy's 5A and Dulbecco's Modified Eagle Medium (DMEM) containing 10% fetal bovine serum and other reagents for cell culture were obtained from Life Technologies (Rockville, MD). 8-

Bromoguanosine 3', 5'-cyclic monophosphate (8-Br-cGMP), a cell-permeant analog of cGMP, was obtained from Sigma (St. Louis, MO) and 500 μ M was used in all experiments (18,20,25,26,34).

Cell lines

C57BL/6-derived EL4 lymphoma cells (lymphoblasts in mouse thymus; thymoma), C57BL/6-derived B16 melanoma cells, and HCT116 (wild-type p53) human colon cancer cells, which lack GUCY2C (Supplementary Fig. 4) (19,34,35), were obtained from ATCC (Manassas, VA). Isogenic HCT116-p53-null cells were a gift from Dr. Bert Vogelstein (Johns Hopkins University, MD) (36). Cell lines were authenticated employing established transcriptomic, proteomic, phenotypic and functional characteristics. Cell stocks were refreshed after the earlier of 10 passages or two years, and were screened for mycoplasma contamination every 6 months with the Universal Mycoplasma Detection Kit (ATCC). Cell lines were obtained and used in 2010-2011.

Ectopic tumor seeding and growth measurement

EL4 and B16 cells (10^4 cells per injection) were injected subcutaneously in mouse flanks (EL4, left and B16, right). Tumor growth was measured once every 3 d and tumor volume was calculated by multiplying 3 tumor dimensions. No significant differences in tumor growth before and after subtotal body irradiation was observed in mice treated with ST compared to CP.

Immunoblot analyses

Protein was extracted from mouse small intestine and colon mucosa in T-Per reagent (Pierce, Dallas, TX), or from *in vitro* cell lysates in Laemmli buffer, and supplemented with protease and phosphatase inhibitors (Roche, Indianapolis, IN). Protein was quantified by immunoblot analysis employing antibodies to: phosphorylated histone H2AX (cat. # 2577, 1:200 dilution), phosphorylated p53 (cat. # 9284, 1:200 dilution), cleaved caspase 3 (cat. # 9579, 1:200 dilution),

Mdm2 (cat. # 3521, 1:200 dilution), and GAPDH (cat. # 2118, 1:200 dilution) from Cell Signaling Technology (Danvers, MA), phosphorylated histone H2AX (cat. #05-636, 1:1000 dilution) from Millipore (Billerica, MA), and p53 (cat. # sc-126, 1:1000 dilution) from Santa Cruz (Santa Cruz, CA). The antibody to GUCY2C was validated previously (25,26). Antisera to GUCA2A and GUCA2B were generously provided by Dr. Michael Goy (University of North Carolina, Chapel Hill, NC) (37,38). Secondary antibodies conjugated to horseradish peroxidase were from Jackson ImmunoResearch Laboratories (West Grove, PA). Staining intensity of specific bands quantified by densitometry was normalized to that for GAPDH using a Kodak imaging system. Average relative intensity reflects the mean of at least three animals in each group and the mean of at least two independent experiments. Molecular weight markers (Cat. # 10748010, 5 μ L per run, or Cat. #LC5800, 10 μ L per run) for immunoblot analyses were from Invitrogen (Grand Island, NY). Secondary antibodies specific to light chains, including goat anti-mouse IgG (cat. # 115-065-174) and mouse anti-rabbit IgG (cat. # 211-062-171), were from Jackson ImmunoResearch Laboratories (Suffolk, UK) for immunoblot analysis following immunoprecipitation.

Immunoprecipitation

Protein from 8-10 x 10⁶ HCT116 cells was extracted in 1% NP40 immunoprecipitation (IP) lysis buffer supplemented with protease and phosphatase inhibitors and incubated with antibodies to Mdm2 (cat. # 3521, 5 μ g) from Cell Signaling Technology and p53 (cat. # sc-126, 1 μ g) from Santa Cruz and protein A beads (Invitrogen, Grand Island, NY) overnight followed by six washes. Precipitated proteins were collected in Laemmli buffer (with 5% beta mercaptoethanol) supplemented with protease and phosphatase inhibitors (Roche) and quantified by immunoblot analysis employing antibodies to Mdm2 (cat. # 3521, 1:200 dilution) from Cell Signaling

Technology and p53 (cat. # sc-126, 1:1000 dilution) from Santa Cruz. Mouse IgG (5 μ g, cat. # 10400C, Invitrogen) and rabbit IgG (5 μ g, cat. # 10400C, Invitrogen) were isotype controls for immunoprecipitation.

Immunohistochemistry and immunofluorescence

Antigens were unmasked in paraffin-embedded sections (5 μ m) by heating at 100° C for 10 min in 10 mM citric buffer, pH 6.0. In addition to those already described, antibodies to antigens probed here included: phosphorylated histone H2AX from Cell Signaling (cat. # 2577, 1:200 dilution), or from Millipore (cat. #05-636, 1:1000 dilution), cleaved caspase 3 from Cell Signaling (cat. # 9579, 1:200 dilution), and β -catenin from Santa Cruz (cat. # sc-7199, 1:50 dilution). The antibody to GUCY2C (25,26) and the antisera to GUCA2A and GUCA2B were described previously (37,38). Fluorescent secondary antibodies were from Invitrogen. Tyramide signal amplification was used to detect GUCY2C and GUCA2A; secondary antibodies conjugated to horseradish peroxidase were from Jackson ImmunoResearch Laboratories (cat #115-035-206 and #111-036-046, 1:1000 dilution), and fluorescein-conjugated tyramine was prepared from tyramine HCl (cat #T2879, Sigma) and NHS-fluorescein (cat #46410, Thermo Scientific) (39). Phosphorylated histone H2AX-positive cells were quantified in 200-1000 crypts per section per animal and positive cells normalized to crypt number. Results reflect the means \pm SEM of at least 3 animals in each group. Immunofluorescence stains were performed in HCT116 and HCT116 p53-null cells using antibodies to the following antigens included: α/β -tubulin from Cell Signaling (cat. # 2148, 1:200 dilution) and γ -tubulin from Abcam (cat. #ab11317, 1:100 dilution, Cambridge, MA). Fluorescence images were captured with an EVOS FL auto cell imaging system from Life Technologies-Thermo Fischer Scientific (Waltham, MA).

Cell treatment, irradiation and colony formation assay

HCT116 and HCT116 p53-null cells were plated in 6-well dishes at 1×10^4 cells/well followed by treatment for 7 d with vehicle or cell permeable cGMP (8-Br-cGMP, 500 μ M). Media containing different treatments were changed every other day. After exposure to radiation (0-4 Gy) cells were trypsinized and plated in 6-well dishes at different densities depending on the potency of the treatments (10^4 cells/well for HCT116 exposed at 0, 1 and 2 Gy; 4×10^4 cells/well for HCT116 p53-null exposed at 0, 1 and 2 Gy; 50×10^4 cells/well for HCT116 exposed at 3 and 4 Gy; 200×10^4 cells/well for HCT116 p53-null exposed at 3 and 4 Gy). Cells were treated with vehicle or 8-Br-cGMP for 7 d after irradiation, then fixed and stained with 10% methylene blue in 70% ethanol. The number of colonies, defined as >50 cells/colony were counted, and the surviving fraction was calculated as the ratio of the number of colonies in the treated sample to the number of colonies produced by cells that were not irradiated. Triplicates were used for each condition in three independent experiments.

Anaphase bridge index (ABI) and aneuploidy

Cells preconditioned with 8-Br-cGMP, or control cells, were irradiated (5 Gy), then seeded on coverslips in 24-well plates (5×10^4 cells per well). ABI and aneuploidy were quantified 2 d after irradiation.

ABI: Cells were fixed in 4% PFA and stained with DAPI. Anaphase cells were analyzed and abnormal anaphase cells were calculated under a fluorescence microscope. More than 200 anaphase cells were analyzed in each treatment group in each independent experiment. Any abnormal anaphase cells with anaphase bridges or anaphase lag showing extended chromosome bridging between two spindle poles were enumerated and the ABI was calculated as percentage

of abnormal anaphase cells over total anaphase cells.

Aneuploidy: Cells were fixed in 4% PFA and stained with DAPI, and immunofluorescence stains were performed using α/β -tubulin-specific antibodies and centromere-specific γ -tubulin antibodies, detected with Alexa Fluor[®] 555 or Alexa Fluor[®] 488 labeled secondary antibodies from Invitrogen. Images were acquired with a laser confocal microscope (Zeiss 510M and Nikon C1 Plus, Thomas Jefferson University Bioimaging Shared Resource), and 0.5 μ m optical sections in the z axis were collected with a 100 \times 1.3 NA oil immersion objective at room temperature. Iterative restoration was performed using LSM Image Browser (Zeiss), and images represent three to four merged planes in the z axis. Abnormal anaphase chromatids were counted if cells contained more than two centrosomes or two centrosomes located in the same direction to the spindle midzone separated from kinetochores at the poles.

Quantitative RT-PCR analysis

Transcripts for GUCY2C, GUCA2A, and GUCA2B were quantified by RT-PCR employing primers and conditions described previously (25,26).

¹²⁵I-labeled ST binding

Binding of ¹²⁵I-labeled ST to GUCY2C was performed as described previously (33). Briefly, membranes were prepared from cells as described previously (33) and ST was iodinated (¹²⁵I-Tyr₄-ST) to a final specific activity of 2,000 Ci/mmol (33). Total binding was measured by counts per minute (CPM) in the absence of unlabeled ST competition, whereas nonspecific binding was measured in the presence of 1 \times 10⁻⁵ M unlabeled ST. Specific binding was calculated by subtracting nonspecific binding from total binding (33). Assays were performed at least in triplicate.

Statistical analyses

Statistical significance was determined by unpaired two-tailed Student's *t* test unless otherwise indicated. Results represent means \pm SEM from at least 3 animals or 3 experiments performed in triplicate. Survival and disease-free survival were analyzed by Kaplan-Meier analysis. Body weight was analyzed using a frailty model combining a segmented linear longitudinal model of body weight, a log-normal model for survival time, and a log-normal model for random break point for body weight (inflection point). Analyses of fecal occult blood and untidy fur were performed by Cochran-Mantel-Hansel test. Colony formation was analyzed by a pairwise comparison in four treatments with isotherm slopes by linear regression.

Results

Silencing GUCY2C exacerbates RIGS. A role for GUCY2C in opposing epithelial cell apoptosis induced by low doses of ionizing radiation (22) suggested that this receptor may play a role in RIGS. Targeted germline deletion of *Gucy2c* (*Gucy2c*^{-/-} mice) (15,16,18-20,26,32) accelerated the death of mice following exposure to a lethal dose (high dose, 15 Gy) of total body irradiation (TBI; Fig. 1A). This dose of radiation produced death by inducing RIGS which could not be rescued by bone marrow transplantation, in contrast to low dose (8 Gy) radiation which produced the hematopoietic, but not the GI, syndrome (Fig. 1B). Similarly, silencing GUCY2C signaling exacerbated acute GI toxicity quantified by diarrhea (Fig. 1C) and decreased survival (Fig. 1D) following 18 Gy sub-total abdominal irradiation (STBI), with bone marrow preservation by shielding. Exacerbation of RIGS in the absence of GUCY2C signaling was associated with increased intestinal dysfunction, including weight loss (Fig. 1E), intestinal bleeding (Fig. 1F), debilitation (untidy fur, Fig. 1G) (40), and stool water accumulation (Fig. 1H) (41). Silencing GUCY2C signaling

amplified intestinal epithelial disruption, quantified as crypt loss, produced by STBI in small intestine (Fig. 1I-J). Moreover, it created novel epithelial vulnerability in the colon, which is relatively resistant to RIGS (Fig. 1K-L) (1-5). Together, these observations reveal that the GUCY2C signaling axis plays a compensatory role in modulating mechanisms contributing to RIGS.

GI-toxic irradiation preserves durable expression of GUCY2C and its paracrine hormones. A role for the GUCY2C paracrine hormone axis in compensatory mechanisms opposing RIGS is predicated on the persistence of expression of the receptor and its hormones following high doses of radiation. Indeed, GUCY2C mRNA and protein, characteristically expressed along the entire crypt-villus axis (17), was durably preserved following lethal TBI (Fig. 2A, B, C), a result that is similar to other conditions disrupting epithelial integrity, including tumorigenesis (18-20,25). Unexpectedly, GI-toxic TBI preserved expression of GUCA2A (Fig. 2D, E, F) and GUCA2B (Fig. 2G, H, I), in contrast to other modes of disrupting epithelial integrity, including tumorigenesis, inflammatory bowel disease, and metabolic stress in which ligand expression is lost (18-21,25,26). Indeed, expression of GUCA2A, which is low in small intestine, was retained primarily in isolated epithelial cells, as described previously (42). In contrast, expression of GUCA2B, which is the predominant GUCY2C hormone in the small intestine, was retained principally by differentiated epithelial cells in distal villi (42). Preservation of receptor and hormone expression was durable, and there were no significant differences in mRNA or protein levels across the time course of injury response (Fig. 2; Supplementary Fig. 5). Moreover, preservation of hormone expression was independent of GUCY2C expression (Supplementary Fig. 6). These observations are consistent with a role for the GUCY2C paracrine hormone signaling axis in compensatory responses that oppose acute radiation-induced GI toxicity. Moreover, the persistence of receptor

expression across the continuum of injury response suggests the potential utility of GUCY2C as a therapeutic target to prevent RIGS.

GUCY2C activation by oral ligand rescues RIGS, but not extra-GI tumor responses to radiation.

In wild type mice, oral administration of ST, an exogenous GUCY2C ligand, reduced morbidity and mortality induced by STBI, quantified by the incidence of diarrhea (Fig. 3A) and survival (Fig. 3B) respectively. Similarly, oral ST opposed STBI-induced intestinal dysfunction, including weight loss (Fig. 3C), intestinal bleeding (Fig. 3D), debilitation (Fig. 3E), and stool water accumulation (Fig. 3F). Further, oral ST rescued intestinal morphology and stool formation (Fig. 3G), and water reabsorption associated with preservation of normal histology (Fig. 3H) after STBI. In contrast, oral ST did not rescue RIGS in *Gucy2c*^{-/-} mice (Supplementary Fig. 7). Furthermore, oral ST did not alter therapeutic radiation responses of radiation-sensitive thymoma or radiation-resistant melanoma (Fig. 3I). Moreover, chronic oral ST was safe, without adverse pharmacological effects like diarrhea (Fig. 3J) or growth retardation (Fig. 3K). These observations support the suggestion that GUCY2C signaling comprises a compensatory mechanism opposing RIGS that can be engaged by orally administered ligands. Indeed, GUCY2C ligands safely protect intestinal epithelial cells specifically (26), without altering therapeutic responses to radiation of tumors outside the intestine.

GUCY2C signaling opposing RIGS requires p53. GUCY2C signaling protects intestinal epithelial cells from apoptosis induced by low dose radiation (22). However, while silencing GUCY2C signaling increased basal levels of apoptosis in small intestine, as demonstrated previously (18), it did not alter apoptosis associated with RIGS along the rostral-caudal axis of the intestine across the continuum of injury responses (Fig. 4A). In that context, p53 also opposes RIGS through

mechanisms that are independent of apoptosis (Supplementary Fig. 8) (7). Indeed, eliminating p53 phenocopied GUCY2C silencing, exacerbating RIGS-related mortality (Fig. 1D; Supplementary Fig. 2). Further, activation of GUCY2C with oral ST improved survival in wild type, but not $p53^{int-/-}$, mice following STBI (Fig. 4B). Moreover, GUCY2C activation opposed STBI-induced intestinal dysfunction quantified by body weight loss (Fig. 4C), intestinal bleeding (Fig. 4D) and debilitation (Fig. 4E) in wild type, but not in $p53^{int-/-}$, mice. These observations suggest that the GUCY2C signaling axis opposes RIGS through a mechanism requiring p53.

GUCY2C signaling opposing RIGS is associated with amplification of p53 responses. Consistent with a role for p53 in mediating the effects of GUCY2C signaling on radiation-induced intestinal toxicity, oral ST increased levels of phosphorylated p53 in mouse intestinal epithelial cells in RIGS induced by STBI (Fig. 4F). Recapitulating these *in vivo* results, the GUCY2C second messenger, cGMP, increased total and phosphorylated p53 induced by radiation in HCT116 human colon carcinoma cells (Fig. 4G), an *in vitro* model of intestinal epithelial cells that express wild type p53, but not GUCY2C (19,34,35) (Supplementary Fig. 4). Amplification of p53 responses to radiation induced by cGMP signaling in HCT116 cells was associated with reduced interactions between p53 and the inhibitory protein Mdm2 (Fig. 4H).

GUCY2C signaling opposing RIGS is associated with p53-dependent rescue of mitotic catastrophe. Induction of GUCY2C signaling by oral ST opposed chromosomal instability in intestinal epithelial cells following STBI, reducing double-strand DNA breaks (Fig. 5A) and abnormal mitoses characteristically associated with mitotic catastrophe (Fig. 5B). Similarly, chromosomal instability produced by irradiation, quantified by centrosome counts or the anaphase bridge index (43), was reduced in HCT116 cells treated with 8-Br-cGMP (Fig. 5C-D). In

contrast, elimination of p53 (HCT116 p53^{-/-}) amplified chromosomal instability produced by irradiation, and this damage was insensitive to 8-Br-cGMP (Fig. 5C-D). Moreover, cell death by mitotic catastrophe reflecting radiation-induced aberrant mitosis was reduced by cGMP in parental, but not in p53^{-/-}, HCT116 cells (Fig. 5E).

DISCUSSION

RIGS reflects radiation-induced genotoxic stress in intestinal epithelial cells (7-9,11,12,14). Radiation produces DNA damage, directly and through reactive oxygen species (23), activating p53 (7,9,14,44). In turn, p53 mediates a bifurcated injury response. Cells damaged beyond repair undergo caspase-dependent apoptosis initiated by p53 activation of PUMA (6,9,12,13). Further, in cells that can be rescued, p53 induces the expression of p21, a key inhibitor of cyclin-dependent kinases which regulates cell cycle checkpoints (7,9,14). Inhibition of proliferation associated with these checkpoints permits cells to repair damaged DNA (7-9,12,14,45). However, p53 responses are limited and cells with damaged DNA escape checkpoints within days of irradiation, enter prematurely into the cell cycle with damaged DNA, and undergo mitotic catastrophe (7,9,12,14,46). In turn, this produces epithelial loss and mucositis, disrupting barrier function associated with fluid and electrolyte loss and infection which are principle mechanisms of death from RIGS (47). Here, we reveal an unexpected compensatory mechanism that opposes this pathophysiology, involving the GUCY2C signaling axis at the intersection of radiation injury and p53 responses.

GUCY2C is selectively expressed by intestinal epithelial cells and activation by the endogenous hormones guanylin and uroguanylin, or the diarrheagenic bacterial STs, increases intracellular cGMP accumulation (17). While there is evidence for GUCY2C signaling in other tissues (32,48),

the effect of oral ST in ameliorating RIGS in the present study is consistent with a primary effect on intestinal receptors, reflecting the absence of bioavailability of oral GUCY2C ligands (31). GUCY2C-cGMP signaling modulates intestinal secretion, one mechanism by which bacteria induce diarrhea, and the oral GUCY2C ligands linaclotide (*Linzess™*) and plecanatide (*Trulance™*) improve constipation and relieve abdominal pain in patients with irritable bowel syndrome (31,49). Further, GUCY2C signaling regulates proliferation and DNA damage repair, processes that are canonically disrupted in RIGS (26). Indeed, signaling through the GUCY2C-cGMP axis inhibits DNA synthesis and prolongs the cell cycle, imposing a G1-S delay in part by regulating p21, key injury responses to radiation (18-20,50). Further, silencing GUCY2C increases DNA oxidation and double strand breaks, amplifying mutations induced by chemical or genetic DNA damage, reflecting ROS and inadequate repair (20). Moreover, silencing GUCY2C disrupts the intestinal barrier (26), a key pathophysiological mechanism contributing to RIGS (47). Conversely, GUCY2C ligands block that damage, enhancing barrier integrity and accelerating recovery from injury (23,24,26,27,30). This role in promoting mucosal barrier integrity supports GUCY2C as a therapeutic target for RIGS.

The present observations suggest a previously unrecognized compensatory mechanism opposing RIGS in which the paracrine hormones guanylin and uroguanylin activate GUCY2C-cGMP signaling to defend the integrity of the intestinal epithelial barrier. In that model, paracrine hormone stimulation of the GUCY2C-cGMP signaling axis supports p53 responses to radiation injury by disrupting interactions with Mdm2, a key regulator of responses to genotoxic stress which binds to the amino terminal of 18-19.p53, inhibiting its transactivation function and targeting it for proteasomal degradation (45,51,52). In turn, amplified p53 responses contribute to resolving

DNA damage, limiting mitotic catastrophe (7). Beyond these compensatory responses, the durable preservation of GUCY2C expression following high dose irradiation across the rostral-caudal axis of the intestine and the continuum of injury responses offers an opportunity to target this receptor for mitigation of RIGS by oral GUCY2C hormone administration. Indeed, it creates the unique possibility of transforming RIGS from a syndrome of irreversible DNA damage to one that can be reversed or prevented by oral GUCY2C ligand supplementation.

These studies stand in contradistinction to other models of intestinal injury in which homeostasis is disrupted through paracrine hormone loss silencing GUCY2C. Indeed, guanylin and uroguanylin are the most commonly lost gene products in sporadic colorectal cancer and these hormones are lost at the earliest stages of neoplasia (29,53,54). Hormone loss silences the GUCY2C signaling axis and interrupts canonical homeostatic mechanisms that regulate the continuously regenerating intestinal epithelium and whose disruption is essential for tumorigenesis (17-20,25,26,34). Similarly, while obesity and colorectal cancer are associated, underlying mechanisms have remained unclear. Recent studies revealed that over-consumption of calories, which is an essential mechanism contributing to obesity, produces ER stress leading to guanylin loss silencing the GUCY2C tumor suppressor (25). Indeed, replacing guanylin suppressed by calories eliminated tumorigenesis (25). Moreover, oral dextran sulfate injures intestinal mucosa, producing inflammatory bowel disease (IBD), and silencing GUCY2C amplifies injury in IBD, increasing mortality in mice (24,26,30). Indeed, IBD is associated with GUCY2C paracrine hormone loss in humans (21). In the context of this emerging paradigm of intestinal epithelial injury, the present results demonstrating the preservation of paracrine hormone expression in

the context of high dose irradiation was unexpected. However, they are consistent with a role for the GUCY2C paracrine hormone axis in compensatory mechanisms opposing RIGS.

Previous studies revealed that silencing GUCY2C amplified apoptosis induced by low doses of radiation (5 Gy) (22). These radiation doses are below GI-toxic levels which produce RIGS or bone marrow failure. Further, silencing GUCY2C (*Gucy2c*^{-/-} mice) did not alter the induction of apoptosis in small or large intestine in RIGS, in contrast to those earlier studies (see Fig. 4A). Moreover, silencing GUCY2C recapitulated the effects of eliminating p53 signaling (*p53*^{-/-} mice), which also had no effect on apoptosis in small or large intestine in RIGS as reported previously (see Supplementary Fig. 8) (7). In the context of the role of GUCY2C in optimizing p53 injury responses, reinforced by the ability of *Gucy2c*^{-/-} mice to phenocopy *p53*^{-/-} mice (see Supplementary Fig. 2) (7), the primary mechanism amplifying epithelial disruption in RIGS in the absence of GUCY2C appears to be mitotic catastrophe, rather than apoptosis.

Targeting p53 directly to prevent and treat RIGS has been uniquely challenging and treatments exploiting this mechanism have not yet emerged (7,9,12,14). The therapeutic challenge arises from the paradoxically opposite roles of p53 in RIGS and the radiation-induced hematopoietic syndrome, the two principal toxicities associated with radiation. Protection of epithelial cells by p53 has made its activation a target to treat RIGS (7-9,14,46). In striking contrast, radiation toxicity mediated by p53 in bone marrow has made its inhibition a target to treat the hematopoietic syndrome (8,46,55). Hence, p53 has remained an elusive target, requiring tissue-specific strategies for appropriate directional regulation. The present study provides insights into novel molecular mechanisms underlying the pathophysiology of RIGS that can be readily translated into p53-targeted medical countermeasures to prevent and treat acute radiation-

induced GI toxicity. Thus, GUCY2C has a narrow tissue distribution, selectively expressed by intestinal epithelial cells from the duodenum to the rectum (15-17). Further, GUCY2C is anatomically privileged, expressed in luminal membranes of those cells, directly accessible to oral agents but inaccessible to the systemic compartment (17,31). Moreover, linaclotide (*Linzess™*) and plecanatide (*Trulance™*) are oral GUCY2C ligands recently approved for the treatment of chronic constipation syndromes, with negligible oral bioavailability or bioactivity outside the GI tract (31). The anatomical privilege of GUCY2C coupled with the compartmentalized activity of linaclotide and plecanatide, confined only to the intestinal lumen, offers a uniquely targeted approach to specifically engage p53-dependent mechanisms, compared to other available approaches, to prevent and treat RIGS. In turn, this offers prophylactic and therapeutic solutions to civilians, first-responders, and military personnel at risk from radiation disasters, like Chernobyl or Fukushima. Similarly, it provides a clinically-tractable approach for targeted prevention of GI toxicity from abdominopelvic radiotherapy for cancer, reducing dose-limiting toxicities and permitting greater radiation fractions to be administered, without altering the therapeutic radiosensitivity of extra-intestinal tumors (see Fig. 3I) (5).

REFERENCES

1. Terry NH, Travis EL. The influence of bone marrow depletion on intestinal radiation damage. *Int J Radiat Oncol Biol Phys* **1989**;17:569-73
2. Mason KA, Withers HR, Davis CA. Dose dependent latency of fatal gastrointestinal and bone marrow syndromes. *Int J Radiat Biol* **1989**;55:1-5

3. Mason KA, Withers HR, McBride WH, Davis CA, Smathers JB. Comparison of the gastrointestinal syndrome after total-body or total-abdominal irradiation. *Radiat Res* **1989**;117:480-8
4. Berger ME, Christensen DM, Lowry PC, Jones OW, Wiley AL. Medical management of radiation injuries: current approaches. *Occup Med (Lond)* **2006**;56:162-72
5. Rodriguez ML, Martin MM, Padellano LC, Palomo AM, Puebla YI. Gastrointestinal toxicity associated to radiation therapy. *Clin Transl Oncol* **2010**;12:554-61
6. Jeffers JR, Parganas E, Lee Y, Yang C, Wang J, Brennan J, *et al.* Puma is an essential mediator of p53-dependent and -independent apoptotic pathways. *Cancer Cell* **2003**;4:321-8
7. Kirsch DG, Santiago PM, di Tomaso E, Sullivan JM, Hou WS, Dayton T, *et al.* p53 controls radiation-induced gastrointestinal syndrome in mice independent of apoptosis. *Science* **2010**;327:593-6
8. Komarova EA, Kondratov RV, Wang K, Christov K, Golovkina TV, Goldblum JR, *et al.* Dual effect of p53 on radiation sensitivity in vivo: p53 promotes hematopoietic injury, but protects from gastro-intestinal syndrome in mice. *Oncogene* **2004**;23:3265-71
9. Leibowitz BJ, Qiu W, Liu H, Cheng T, Zhang L, Yu J. Uncoupling p53 functions in radiation-induced intestinal damage via PUMA and p21. *Molecular cancer research : MCR* **2011**;9:616-25
10. Paris F, Fuks Z, Kang A, Capodiceci P, Juan G, Ehleiter D, *et al.* Endothelial apoptosis as the primary lesion initiating intestinal radiation damage in mice. *Science* **2001**;293:293-7

11. Potten CS. Radiation, the ideal cytotoxic agent for studying the cell biology of tissues such as the small intestine. *Radiat Res* **2004**;161:123-36
12. Qiu W, Carson-Walter EB, Liu H, Epperly M, Greenberger JS, Zambetti GP, *et al.* PUMA regulates intestinal progenitor cell radiosensitivity and gastrointestinal syndrome. *Cell Stem Cell* **2008**;2:576-83
13. Villunger A, Michalak EM, Coultas L, Mullauer F, Bock G, Ausserlechner MJ, *et al.* p53- and drug-induced apoptotic responses mediated by BH3-only proteins puma and noxa. *Science* **2003**;302:1036-8
14. Sullivan JM, Jeffords LB, Lee CL, Rodrigues R, Ma Y, Kirsch DG. p21 protects "Super p53" mice from the radiation-induced gastrointestinal syndrome. *Radiat Res* **2012**;177:307-10
15. Schulz S, Green CK, Yuen PS, Garbers DL. Guanylyl cyclase is a heat-stable enterotoxin receptor. *Cell* **1990**;63:941-8
16. Schulz S, Lopez MJ, Kuhn M, Garbers DL. Disruption of the guanylyl cyclase-C gene leads to a paradoxical phenotype of viable but heat-stable enterotoxin-resistant mice. *J Clin Invest* **1997**;100:1590-5
17. Kuhn M. Molecular physiology of membrane guanylyl cyclase receptors. *Physiol Rev* **2016**;96:751-804
18. Li P, Lin JE, Chervoneva I, Schulz S, Waldman SA, Pitari GM. Homeostatic control of the crypt-villus axis by the bacterial enterotoxin receptor guanylyl cyclase C restricts the proliferating compartment in intestine. *Am J Pathol* **2007**;171:1847-58

19. Li P, Schulz S, Bombonati A, Palazzo JP, Hyslop TM, Xu Y, *et al.* Guanylyl cyclase C suppresses intestinal tumorigenesis by restricting proliferation and maintaining genomic integrity. *Gastroenterology* **2007**;133:599-607
20. Lin JE, Li P, Snook AE, Schulz S, Dasgupta A, Hyslop TM, *et al.* The hormone receptor GUCY2C suppresses intestinal tumor formation by inhibiting AKT signaling. *Gastroenterology* **2010**;138:241-54
21. Brenna O, Bruland T, Furnes MW, Granlund A, Drozdov I, Emgard J, *et al.* The guanylate cyclase-C signaling pathway is down-regulated in inflammatory bowel disease. *Scand J Gastroenterol* **2015**;50:1241-52
22. Garin-Laflam MP, Steinbrecher KA, Rudolph JA, Mao J, Cohen MB. Activation of guanylate cyclase C signaling pathway protects intestinal epithelial cells from acute radiation-induced apoptosis. *Am J Physiol Gastrointest Liver Physiol* **2009**;296:G740-9
23. Han X, Mann E, Gilbert S, Guan Y, Steinbrecher KA, Montrose MH, *et al.* Loss of guanylyl cyclase C (GCC) signaling leads to dysfunctional intestinal barrier. *PLoS One* **2011**;6:e16139
24. Harmel-Laws E, Mann EA, Cohen MB, Steinbrecher KA. Guanylate cyclase C deficiency causes severe inflammation in a murine model of spontaneous colitis. *PLoS One* **2013**;8:e79180
25. Lin JE, Colon-Gonzalez F, Blomain E, Kim GW, Aing A, Stoecker B, *et al.* Obesity-induced colorectal cancer is driven by caloric silencing of the guanylin-GUCY2C paracrine signaling axis. *Cancer Res* **2016**;76:339-46

26. Lin JE, Snook AE, Li P, Stoecker BA, Kim GW, Magee MS, *et al.* GUCY2C opposes systemic genotoxic tumorigenesis by regulating AKT-dependent intestinal barrier integrity. *PLoS One* **2012**;7:e31686
27. Mann EA, Harmel-Laws E, Cohen MB, Steinbrecher KA. Guanylate cyclase C limits systemic dissemination of a murine enteric pathogen. *BMC Gastroenterol* **2013**;13:135
28. Shailubhai K, Palejwala V, Arjunan KP, Saykhedkar S, Nefsky B, Foss JA, *et al.* Plecanatide and dolcanatide, novel guanylate cyclase-C agonists, ameliorate gastrointestinal inflammation in experimental models of murine colitis. *World J Gastrointest Pharmacol Ther* **2015**;6:213-22
29. Shailubhai K, Yu HH, Karunanandaa K, Wang JY, Eber SL, Wang Y, *et al.* Uroguanylin treatment suppresses polyp formation in the Apc(Min/+) mouse and induces apoptosis in human colon adenocarcinoma cells via cyclic GMP. *Cancer Res* **2000**;60:5151-7
30. Steinbrecher KA, Harmel-Laws E, Garin-Laflam MP, Mann EA, Bezerra LD, Hogan SP, *et al.* Murine guanylate cyclase C regulates colonic injury and inflammation. *J Immunol* **2011**;186:7205-14
31. Camilleri M. Guanylate cyclase C agonists: emerging gastrointestinal therapies and actions. *Gastroenterology* **2015**;148:483-7
32. Valentino MA, Lin JE, Snook AE, Li P, Kim GW, Marszalowicz G, *et al.* A uroguanylin-GUCY2C endocrine axis regulates feeding in mice. *J Clin Invest* **2011**;121:3578-88
33. Waldman SA, Barber M, Pearlman J, Park J, George R, Parkinson SJ. Heterogeneity of guanylyl cyclase C expressed by human colorectal cancer cell lines in vitro. *Cancer Epidemiol Biomarkers Prev* **1998**;7:505-14

34. Gibbons AV, Lin JE, Kim GW, Marszalowicz GP, Li P, Stoecker BA, *et al.* Intestinal GUCY2C prevents TGF-beta secretion coordinating desmoplasia and hyperproliferation in colorectal cancer. *Cancer Res* **2013**;73:6654-66
35. Zuzga DS, Pelta-Heller J, Li P, Bombonati A, Waldman SA, Pitari GM. Phosphorylation of vasodilator-stimulated phosphoprotein Ser239 suppresses filopodia and invadopodia in colon cancer. *Int J Cancer* **2012**;130:2539-48
36. Bunz F, Dutriaux A, Lengauer C, Waldman T, Zhou S, Brown JP, *et al.* Requirement for p53 and p21 to sustain G2 arrest after DNA damage. *Science* **1998**;282:1497-501
37. Li Z, Taylor-Blake B, Light AR, Goy MF. Guanylin, an endogenous ligand for C-type guanylate cyclase, is produced by goblet cells in the rat intestine. *Gastroenterology* **1995**;109:1863-75
38. Perkins A, Goy MF, Li Z. Uroguanylin is expressed by enterochromaffin cells in the rat gastrointestinal tract. *Gastroenterology* **1997**;113:1007-14
39. Faget L, Hnasko TS. Tyramide signal amplification for immunofluorescent enhancement. *Methods Mol Biol* **2015**;1318:161-72
40. Moreau MR, Wijetunge DS, Bailey ML, Gongati SR, Goodfield LL, Hewage EM, *et al.* Growth in egg yolk enhances salmonella enteritidis colonization and virulence in a mouse model of human colitis. *PLoS One* **2016**;11:e0150258
41. Fierer J, Okamoto S, Banerjee A, Guiney DG. Diarrhea and colitis in mice require the Salmonella pathogenicity island 2-encoded secretion function but not SifA or Spv effectors. *Infect Immun* **2012**;80:3360-70

42. Brenna O, Furnes MW, Munkvold B, Kidd M, Sandvik AK, Gustafsson BI. Cellular localization of guanylin and uroguanylin mRNAs in human and rat duodenal and colonic mucosa. *Cell Tissue Res* **2016**;365:331-41
43. Ganem NJ, Godinho SA, Pellman D. A mechanism linking extra centrosomes to chromosomal instability. *Nature* **2009**;460:278-82
44. Marusyk A, Casas-Selves M, Henry CJ, Zaberezhnyy V, Klawitter J, Christians U, *et al.* Irradiation alters selection for oncogenic mutations in hematopoietic progenitors. *Cancer Res* **2009**;69:7262-9
45. Vousden KH, Prives C. Blinded by the Light: The growing complexity of p53. *Cell* **2009**;137:413-31
46. Lee CL, Blum JM, Kirsch DG. Role of p53 in regulating tissue response to radiation by mechanisms independent of apoptosis. *Translational cancer research* **2013**;2:412-21
47. Hauer-Jensen M, Denham JW, Andreyev HJ. Radiation enteropathy--pathogenesis, treatment and prevention. *Nature reviews Gastroenterology & hepatology* **2014**;11:470-9
48. Carrithers SL, Hill MJ, Johnson BR, O'Hara SM, Jackson BA, Ott CE, *et al.* Renal effects of uroguanylin and guanylin in vivo. *Brazilian journal of medical and biological research = Revista brasileira de pesquisas medicas e biologicas* **1999**;32:1337-44
49. Castro J, Harrington AM, Hughes PA, Martin CM, Ge P, Shea CM, *et al.* Linaclotide inhibits colonic nociceptors and relieves abdominal pain via guanylate cyclase-C and extracellular cyclic guanosine 3',5'-monophosphate. *Gastroenterology* **2013**;145:1334-46 e1-11

50. Basu N, Saha S, Khan I, Ramachandra SG, Visweswariah SS. Intestinal cell proliferation and senescence are regulated by receptor guanylyl cyclase C and p21. *The Journal of biological chemistry* **2014**;289:581-93
51. Chene P. Inhibiting the p53-MDM2 interaction: an important target for cancer therapy. *Nature reviews Cancer* **2003**;3:102-9
52. Prives C. Signaling to p53: breaking the MDM2-p53 circuit. *Cell* **1998**;95:5-8
53. Wilson C, Lin JE, Li P, Snook AE, Gong J, Sato T, *et al.* The paracrine hormone for the GUCY2C tumor suppressor, guanylin, is universally lost in colorectal cancer. *Cancer Epidemiol Biomarkers Prev* **2014**;23:2328-37
54. Steinbrecher KA, Tuohy TM, Heppner Goss K, Scott MC, Witte DP, Groden J, *et al.* Expression of guanylin is downregulated in mouse and human intestinal adenomas. *Biochem Biophys Res Commun* **2000**;273:225-30
55. Lotem J, Sachs L. Hematopoietic cells from mice deficient in wild-type p53 are more resistant to induction of apoptosis by some agents. *Blood* **1993**;82:1092-6

FIGURE LEGENDS

Figure 1. GUCY2C silencing amplifies RIGS. (A) *Gucy2c*^{-/-} mice are more susceptible to death, compared to *Gucy2c*^{+/+} mice, induced by high dose (15 Gy) whole body irradiation (TBI, Kaplan-Meier analysis, *** p<0.001; n=34 *Gucy2c*^{+/+} mice, n=39 *Gucy2c*^{-/-} mice). **(B)** Mortality from low dose (8 Gy) TBI reflected hematopoietic toxicity, which was abrogated by bone marrow transplantation (BMT). In contrast, mortality from high dose TBI (15 Gy) reflected both hematopoietic and GI toxicity which could not be rescued by BMT [Kaplan-Meier analysis, *** p<0.001 between *Gucy2c*^{+/+} mice (n=11) and *Gucy2c*^{+/+} mice with BMT (n=5) following low dose (8 Gy) TBI; p<0.05 (not significant) between *Gucy2c*^{+/+} mice (n=21) and *Gucy2c*^{+/+} mice with BMT (n=15) following high dose TBI]. Following 18 Gy STBI, *Gucy2c*^{-/-} mice were more susceptible to diarrhea **(C)**, Chi-square test, two sided, * p<0.05), mortality **(D)**, Kaplan-Meier analysis, ** p<0.01), weight loss **(E)**, Frailty model analysis, * p<0.05), intestinal bleeding **(F)**, fecal occult blood; FOB; Cochran-Mantel-Haenszel test, * p<0.05), debilitation **(G)**, untidy fur; Cochran-Mantel-Haenszel test, * p<0.05), and stool water accumulation **(H)**, Loess smoothing curves with 95% confidence bands and comparison of area under curve (AUC), * p<0.05; dashed line indicates stool water content before irradiation]. **(I-L)** *Gucy2c*^{-/-} mice were more susceptible to radiation-induced GI injury in both small **(I-J)** and large **(K-L)** intestines quantified by crypt enumeration post irradiation (15 Gy TBI), compared to *Gucy2c*^{+/+} mice (ANOVA, * p<0.05, ** p<0.01, n_≥3 *Gucy2c*^{+/+} and *Gucy2c*^{-/-} mice, respectively, at each time point). Bars in low power images represent 500 μm, and in high power images 50 μm, in **I** and **K**. n=34 *Gucy2c*^{+/+} mice, n=35 *Gucy2c*^{-/-} mice in **C-E** and **G**; n=13 *Gucy2c*^{+/+} mice, n=13 *Gucy2c*^{-/-} mice in **F**; n=26 *Gucy2c*^{+/+} mice and n=28 *Gucy2c*^{-/-} mice in **H**.

Figure 2. The GUCY2C hormone axis is preserved in RIGS. (A-F) TBI (15 Gy) did not significantly alter the relative expression of (A) GUCY2C, (D) guanylin (GUCA2A), or (G) uroguanylin (GUCA2B) mRNA or (B) GUCY2C, (E) GUCA2A, or (H) GUCA2B protein in jejunum over time [n=4-8 per time point; $p>0.05$ (not significant) for mRNA or protein by ANOVA]. (C, F, I) Representative immunofluorescence images for the expression of GUCY2C, GUCA2A, and GUCA2B before and 48 h after 15 Gy TBI [green, GUCY2C; red, hormone (GUA2A, GUCA2B); blue, DAPI]. Bar represents 50 μm .

Figure 3. Oral ST selectively opposes RIGS. (A-F) *Gucy2c*^{+/+} mice preconditioned with oral ST for 14 d prior to and following 18 Gy STBI (on d 0), exhibited a lower incidence of diarrhea (A) induced by STBI, compared to mice treated with control peptide (CP) (Fisher's exact test, two sided, * $p<0.05$). Similarly, following 18 Gy STBI, ST improved (B) diarrhea-free survival (Kaplan-Meier survival analysis, ** $p<0.01$); (C) weight loss and weight recovery (Frailty model analysis, * $p<0.05$); (D) FOB and (E) untidy fur (Cochran-Mantel-Haenszel test, * $p<0.05$); and (F) stool water content [Loess smoothing curves with 95% confidence bands and comparison of area under curve (AUC), *** $p<0.001$; dashed line, stool water content before irradiation]. (G-H) ST reduced radiation-induced intestinal damage 15 d following STBI, reflected by (G) gross morphology, with lower hyperemia, edema, and unformed stool, and (H) histology, without disruption of normal crypt-villus architecture quantified by crypt depth, stromal hypertrophy reflected by intestinal transmural thickness and lymphocytic infiltration (Fisher's exact test, two sided, * $p<0.05$ in G; t-test, two sided, *** $p<0.001$ in H; n=4 CP-treated mice, n=5 ST-treated mice). Bar in H represents 100 μm . (I) Oral ST did not alter radiation responses by subcutaneous thymoma or melanoma (t test, two sided, $p>0.05$; dashed line, original tumor size). (J-K) Chronic (>2 weeks) oral ST did not

produce diarrhea (J) or growth retardation (K) ($p > 0.05$, ANOVA). In A-F and I-K, $n = 9$ CP-treated mice, $n = 9$ ST-treated mice.

Figure 4. GUCY2C signaling amplifies p53 response to RIGS by disrupting p53-Mdm2 interaction.

(A) Silencing GUCY2C did not affect apoptosis induced by 15 Gy TBI in small intestine and colon (t-test, two sided, $* p < 0.05$; *Gucy2c*^{-/-} mice, $n \geq 3$ and *Gucy2c*^{+/+} mice, $n \geq 3$ at each time point). Oral ST improved (B) diarrhea-free survival [Kaplan-Meier analysis, $** p < 0.01$ between *p53*^{int+/+} mice treated with CP ($n = 17$) or ST ($n = 16$); $p > 0.05$ between *p53*^{int-/-} mice treated with CP ($n = 11$) or ST ($n = 11$)]; (C) weight [Frailty model analysis, $* p < 0.05$ between *p53*^{int+/+} mice treated with CP ($n = 17$) or ST ($n = 16$); $p > 0.05$ between *p53*^{int-/-} mice treated with CP ($n = 11$) or ST ($n = 11$)]; and (D) FOB and (E) untidy fur [Cochran-Mantel-Haenszel test, $* p < 0.05$ between *p53*^{int+/+} mice treated with CP ($n = 17$) or ST ($n = 16$); $p > 0.05$ between *p53*^{int-/-} mice treated with CP ($n = 11$) or ST ($n = 11$)] following 18 Gy STBI in *p53*^{int+/+}, but not *p53*^{int-/-}, mice. (F) Oral ST promoted p53 phosphorylation in small intestine 7 d after 18 Gy STBI (t-test, two sided, $* p < 0.05$, $n = 6$ in CP and $n = 6$ in ST treated mice). Bar represents 50 μm . (G) 8-Br-cGMP increased total and phosphorylated p53 in response to 5 Gy radiation in HCT116 human colon carcinoma cells ($n \geq 3$ in each treatment group; $* p < 0.05$, $** p < 0.01$, ANOVA). (H) 8-Br-cGMP increased p53 activation in HCT116 cells in response to 5 Gy radiation by disrupting p53-Mdm2 interaction, quantified by immunoprecipitation (IP) and Western Blot (WB) with antibodies to p53 or Mdm2 ($n \geq 3$ in each group; $* p < 0.05$, $** p < 0.01$, ANOVA). Mouse and rabbit IgG was used as isotype controls in (H).

Figure 5. GUCY2C signaling requires p53 to oppose mitotic catastrophe. (A)

Oral ST reduced DNA double strand breaks (γ -H2AX; t-tests, two sided, $*** p < 0.001$, $n = 4$ mice treated with CP treated, $n = 5$ mice treated with ST; > 200 crypts were examined in each mouse) and (B) abnormal mitotic

orientation [(%) of metaphase plates oriented non-orthogonally to the crypt-surface axis]] (t-tests, two sided, * $p < 0.05$; $n = 4$ mice treated with CP treated, $n = 5$ mice treated with ST; ≥ 50 mitotic figures were evaluated in each mouse intestine) following 18 Gy STBI (red, β -catenin; green, γ -H2AX; blue, DAPI). Bars represent 50 μm . **(C)** Radiation (5 Gy)-induced anaphase bridging, a marker of abnormal mitosis quantified by the anaphase bridge index (ABI), in wild type (parental) and p53-null (p53^{-/-}) HCT116 human colon carcinoma cells, was reduced by pretreatment with a cell-permeant analogue of cGMP in a p53-dependent fashion. Representative images of ABI: i, normal mitosis without anaphase bridge, ii-iii, abnormal mitoses with anaphase bridges (Chi-square tests, two sided, * $p < 0.05$; ≥ 100 cells in anaphase were examined in each group). **(D)** Radiation (5 Gy)-induced aneuploidy, quantified by centrosome enumeration, in parental and p53-null HCT116 cells, was reduced in a p53-dependent fashion by pretreatment with 8-Br-cGMP. Representative images of ploidy: i, normal diploidy, ii, abnormal diploidy, iii, triploidy, iv, tetraploidy. (red, α/β -tubulin; green, γ -tubulin; purple, DAPI) (Chi-square tests, two sided, *** $p < 0.001$, ≥ 200 mitotic cells were examined in each group). **(E)** Cytogenetic toxicity induced by increasing doses of radiation, quantified by colony formation, in parental and p53-null HCT116 cells was reduced in a p53-dependent fashion by pretreatment with 8-Br-cGMP [Pairwise comparison of isotherm slopes, * $p < 0.05$: HCT116 cells treated with cGMP compared to the three other groups including HCT116 cells treated with PBS, HCT116 p53-null cells treated with PBS or cGMP; $p > 0.05$ (not significant) between any two of these three latter groups].